
A new strategy to evaluate aptamer binding affinity

R. Cataldo^{1,4,*}, F. Ciriaco^{2,*}, E. Alfinito^{3,4,*}

¹Department of Mathematics and Physics, "Ennio de Giorgi", University of Salento, Via Monteroni, Lecce, Italy, I-7310,

²Department of Chemistry, University of Bari, Via Orabona 4, Bari, Italy, I-70126,

³Department of Innovation Engineering, University of Salento, Via Monteroni, Lecce, Italy, I-73100

⁴Istituto Nazionale di Fisica Nucleare, INFN, sezione di Lecce, Italy

*To whom correspondence should be addressed.

Abstract

Motivation: The selection of high-affinity aptamers is of paramount interest for clinical and technological applications. A computational investigation to evaluate the relative binding ability of a group of anti-Angiopoietin-2 aptamers is proposed and tested against data already available in the literature.

Results: The procedure consists of three steps: a. the production of a large set of conformations for each candidate aptamer; b. the rigid docking upon the receptor; c. the topological and electrical characterization of the products. Steps a and b allow a global binding score of the ligand-receptor complexes, based on the distribution of the "effective affinity", i.e. the sum of the conformational and the docking energies. Step c. employs a complex network approach (Proteotronics) to characterize the electrical properties of the aptamers and the complexes. Finally, a comparison of the theoretical results with the measurements obtained for the same aptamers in experiments on the SPR biosensor is performed, revealing a good agreement.

Contact: rosella.cataldo@unisalento.it, fulvio.ciriaco@uniba.it, eleonora.alfinito@unisalento.it

1 Introduction

The growing interest in therapeutic aptamers (Lee *et al.*, 2015) is pushing the research for even more efficient and stable macromolecules. The biotechnological approaches, mainly SELEX procedure (Tuerk *et al.*, 1990) involve high costs in materials and time. Therefore, a large number of computational methods and applications in this sector (Chushak *et al.*, 2009; Bini *et al.*, 2011) have been developed, starting from the experience gained in guessing protein sequences and structures (Gilson *et al.*, 2007; Rother *et al.*, 2011). Because of the wide range of size and behaviour of ligands, aptamers as a special case, and of receptors these methods may derive from entirely different concepts and attain varying accuracy (Kitchen *et al.*, 2004).

The affinity of an aptamer for a receptor depends on the reciprocal capability to attain geometrical conformations where the binding functionalities match each other (Kitchen *et al.*, 2004). Therefore, most approaches must cope with the difficulties arising from the treatment of a potentially very large number of masses and interactions: ligand, receptor and possibly solvent atoms and, depending on the size of the problem, introduce some approximations (Stewart *et al.*, 2006). Methods are present in the literature (Kinnings *et al.*, 2011) that completely avoid the geometrical docking problem, relying instead on classification of the ligands on the basis of a large number of molecular descriptors. However, even when a good set of descriptors can be found, the ligand classification must be benchmarked against a large number of known samples.

Renouncing to follow the equations of motion to concentrate only on the recognition of the lowest energy conformations of the ligand/receptor system, docking methods are important representatives of these approaches. In a nutshell, docking generates samples of the conformational space of the system and ranks them. Therefore, both the exhaustiveness of the sampling and the correctness of the ranking function ultimately affect the accuracy of docking (Kitchen *et al.*, 2004).

Hu *et al.* (2015) computationally selected RNA mutant sequences with high affinity for Angiopoietin-2 (Ang2), starting from the sequences of anti-Ang2 aptamers, obtained by the SELEX procedure. Using the ZDOCK program, the Authors of (Hu *et al.*, 2015) carried out simulations of aptamer-protein interactions, scoring the result of each simulation with the ZRANK functions in Discovery Studio 3.5 (DS 3.5; Accelrys Inc., San Diego, USA). To test the prediction accuracy, experimental data were obtained from measurements with a surface plasmon resonance (SPR) biosensor. The three highest ZRANK score mutant sequences along with a high (Seq1) and low (Seq16) affinity binding sequence were analysed. Quite interestingly, one of the mutant structures, named Seq2_12_35, which showed the best ZRANK score among the five-selected aptamer, was one of the worst performing in experiments.

These outcomes highlight the challenge of the *in silico* determination of the three-dimensional (3D) conformation of RNA aptamers and aptamer-

protein complexes. This is significantly more difficult than protein structure determination (Doudna, 2000), so that the majority of known RNAs remain structurally uncharacterized (Boniecki *et al.*, 2016).

Boniecki *et al.* (2016) developed a free software, SimRNA, for computational RNA 3D structure prediction. SimRNA uses a coarse-grained representation of the RNA skeleton. It then relies on Monte Carlo methods for sampling the configurational space, guided by a suitable potential energy, statistically derived from experimental data. For modelling complex 3D structures, the software can use additional constraints, derived from experimental or computational analyses, including information about secondary structure and/or long-range contacts. SimRNA can be also used to analyse configurational landscapes and identify potential alternative structures.

The modelling of the physical properties of biomolecules, that is, electrical transport, conformational change, thermal modes and so on, is a long time debated problem (Tirion, 1996; Baranowski, 2006; Piazza *et al.* 2009), mainly concerned with the level of granularity used for the description. Recently, a novel approach called *Proteotronics*, able to conjugate structure and function of proteins and aptamers at a microscopic level, has been developed (Alfinito *et al.* 2010, 2011, 2015, 2017). The core idea is that structure and function of biomolecules can be described simultaneously, by using a complex network whose degree of connections depends on the biomolecule activation state (Alfinito *et al.* 2010, 2011, 2015, 2017).

Proteotronics, initially developed for proteins, was for the first time tested on the single DNA 15-mer thrombin binding aptamer (TBA) alone and complexed with thrombin, correctly describing and interpreting some relevant results experimentally obtained by using X-ray spectroscopy (Alfinito *et al.*, 2017) and electrochemical measurements. In particular, the model was able to foresee the reduced affinity of the TBA-thrombin complex, when produced in the presence of Na⁺, with respect that of the same compound, produced in a solution containing K⁺. Furthermore, the model revealed that resistance measurements are sensitive to different affinities (Alfinito *et al.*, 2017).

This paper proposes a novel strategy for the screening of a group of aptamers on the basis of their binding affinity for a receptor. This strategy is described and benchmarked in the following points:

- Sampling RNA-aptamer conformations (pre-docking) through an *ad hoc* computational procedure.
- Docking all the previously obtained aptamer sample conformations to the target.
- Capturing some topological and electrical features of the aptamer docked with the target, on the basis of the principles of *Proteotronics*.
- Comparing the theoretical results with experiments (Hu *et al.*, 2015).

The entire proposed procedure shows a satisfactory agreement with the experimental findings, so that it can be considered successfully when used for evaluation of aptamers binding affinity.

2 System and Methods

The method here proposed was applied to the same problem as in (Hu *et al.*, 2015), that is a comparative evaluation of binding to angiopoietin Ang2 of five different aptamers:

1. an aptamer, denoted "Seq1", both in Hu's paper and below, from the pool of Ang2 specific RNA aptamers known in the literature;
2. three mutant sequences, here and in Hu's paper denoted "Seq2_12_35", "Seq15_12_35", and "Seq15_15_38";
3. an Ang1-specific RNA aptamer, denoted "Seq16", as in Hu *et al.*, there applied as a control sample.

2.1 Sampling RNA-aptamer conformations

Among the tools for the prediction of RNA tertiary structure (Dawson *et al.* 2016), SimRNA (Boniecki *et al.*, 2016) was chosen.

SimRNA makes use of a simplified (coarse-grained) representation of the nucleotide chain, consisting of 5-6 dihedral angles for each nucleotide to describe the general aspects of the chain. The program then applies a Monte Carlo scheme for sampling the conformational space, with acceptance and rejection dictated by a function that plays the role of potential energy.

The function prescription is obtained from a large set of crystallographic well resolved structures (Boniecki *et al.*, 2016).

For each prediction, after an initial annealing phase, we carried out four independent runs of the Replica Exchange Monte Carlo simulation (Boniecki *et al.*, 2016), each employing ten replicas.

Then, we performed a clusterization of the obtained structures, based on geometrical similitude, following the procedure drawn in the SimRNA manual (Boniecki *et al.*, 2014).

Sampling the space of ligand conformations allowed us to obtain more stable docked structures than proceeding from the minimum energy conformation. The slideshow in Figure 1 shows a set of Seq1 conformations, all reasonably affordable at room temperature.

By means of the clustering algorithm, from about 30 up to 60 clusters were produced for each studied aptamer. A finer sampling can be obtained tweaking the parameters. The realizations were statistically analysed by proper SimRNA functions, in order to obtain, for each of the five studied aptamers, the frame corresponding to the lowest energy (Boniecki *et al.*, 2014). In doing so, the code permits to establish a lower RMSD threshold, for the first pass of clustering, and a higher RMSD threshold for a second pass of clustering (Boniecki *et al.*, 2014). Usually, those thresholds are about 10% of the number of nucleobases of the sequence. The docking of the aptamers to the receptor was performed by means of AutoDock-Vina (Trott *et al.*, 2010).

The receptor binding domain 1Z3S of Ang2 (Barton *et al.*, 2005) and the aptamers were assigned partial charges and atom types by means of MGLTools.

The backmapping of the SimRNA reduced set of freedom degrees to the full set of atom coordinates was in a few cases unsuccessful: MGLTools in particular did not recognize the reconstructed molecule as a single sequence, due to infringement of geometrical constraints on bond distances. For example, the structure marked * in Figure 1 is broken into two subsequences, both by MGLTools and by PyMol, as visible in those screenshots.

We choose to discard such structures rather than repairing them with *ad hoc* procedures or modifying the binding parameter of MGLTools. MGLTools was also used to translate back the poses obtained from AutoDock-Vina to pdb format.

2.2 The Proteotronics approach

The Proteotronics approach is a theoretical and computational procedure to analyse the physical response of biomaterials in electronic devices. It is a single-macromolecule modelling which takes into account both structure and function of the object, able to describe the macroscopic data as emerging properties due to local interactions. The general strategy rises to the macroscopic physical features, by using a coarse-grained description of the 3D structure. In the literature (Tirion, 1996; Baranowski, 2006; Piazza *et al.* 2009; Alfinito *et al.* 2015), the level of refinement of this description ranges from the complete molecule to the single atom. A good compromise is observed in the case of the single amino-acid level, sufficient to keep most of the information useful for technological applications with the advantage of quite small computational times. This kind of description has been extended to aptamers (Alfinito *et al.* 2017), since the macroscopic mechanism of aptamer binding is quite similar to that observed in proteins.

The procedure has been extensively described in previous papers (Alfinito *et al.* 2010, 2011, 2015, 2017) and consists of three steps:

- The graph analogue building;
- The interaction network building;
- The network solution.

Starting from the 3D structure of the aptamer, the corresponding graph is set up, using the following rules:

1. Each nucleobase (amino acid) is mapped into a single node, whose space position is that of C_1 (C_α) carbon atom as the centroid of the real molecule (Alfinito *et al.* 2015). Two nodes are connected with a link only if their distance is below an assigned interaction radius, R_c . The graph preserves the macromolecule topology.

2. A specific kind of interaction is selected. Here a simple charge transfer in the linear regime is described. Each link is translated into a resistance. In particular, the resistance between a couple of nodes, say a, b , is calculated as that of a cylindrical structure of length $l_{a,b}$, the distance between the nodes, and surface A_{ab} , the intersection area of the spheres of radius R_c , drawn around the nodes.

3. Finally, resistance can be calculated by using appropriate resistivity values, as detailed in (Alfinito *et al.* 2017). A couple of ideal electrodes connects the network to an external bias. The network is solved, for an assigned value of R_c , by using the standard Kirchhoff rules.

3 Results and Discussion

3.1 Effective affinity

For the following discussion we introduce the term "effective affinity" (EA) to indicate

$$EA = E_{\text{docking}} + E_{\text{SimRNA}} \quad (1)$$

A justification is here needed of how we abuse the SimRNA knowledge derived potential to translate it into energetic units and let it contribute to the global ranking.

The SimRNA potential is the guide of Monte Carlo procedure driving the structure from the initial state to the most stable configuration (Boniecki *et al.*, 2016). Therefore, it effectively works ranking the conformations on the

basis of their energy, though a large imprecision has to be expected and perfectly in line with the purpose of the SimRNA potential. The function realization is obtained from scrutiny of a large number of experimental RNA structures, so as to best match the distribution of local configurational motifs of SimRNA *in silico* evolution and the experimental distribution of the same motifs in the selected database.

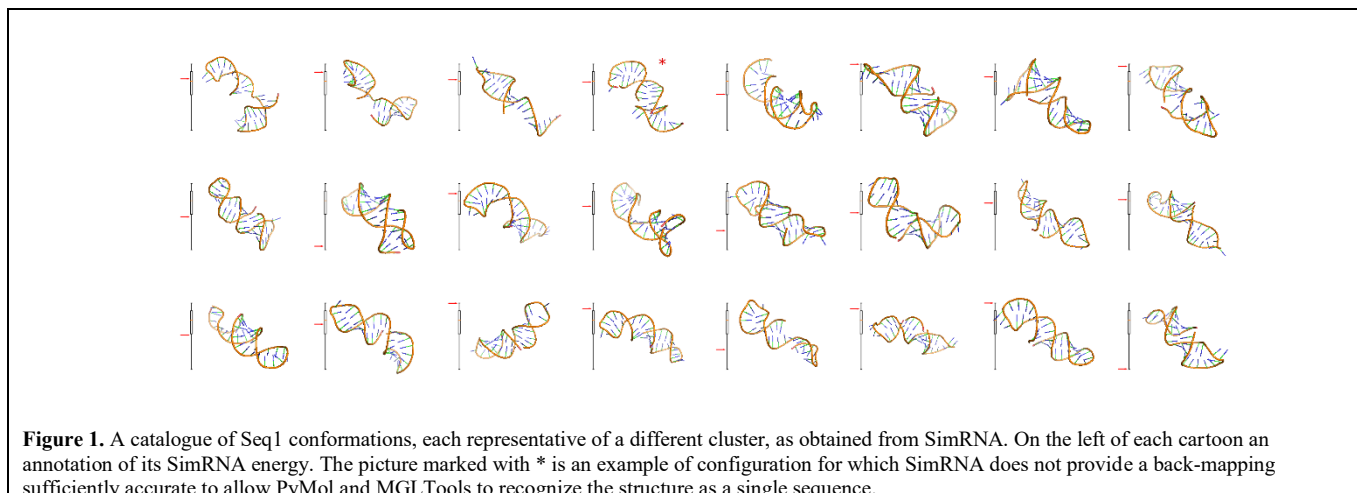


Figure 1. A catalogue of Seq1 conformations, each representative of a different cluster, as obtained from SimRNA. On the left of each cartoon an annotation of its SimRNA energy. The picture marked with * is an example of configuration for which SimRNA does not provide a back-mapping sufficiently accurate to allow PyMol and MGLTools to recognize the structure as a single sequence.

Therefore, we assimilate the SimRNA potential function to a somewhat approximated thermodynamic potential, i.e. deciding the statistical distribution of conformational parameters.

Since most of the experimental structures behind the SimRNA potential are reasonably obtained nearby-room temperatures, we decided to translate the unitless SimRNA energy on the basis of the formula

$$E_{\text{SimRNA}} = E_{\text{unitless}} * RT \quad (2)$$

where R is the gas constant and T=298 K.

Among the thermodynamic measures, the effective affinity should have the closest correspondence with the binding enthalpy.

As approximate as it may be, the SimRNA energy contribution cannot be discarded in the evaluation of ligand affinity, unless one finds a better evaluation of the aptamer conformational energy.

The distribution of docking energies in Figure 2 is meant to illustrate this concept: docking energies much lower than those corresponding to the most stable aptamer conformation are present, others could appear if the sampling procedure were extended so that higher energy conformations are represented.

To put a remedy to the imprecise correspondence of the SimRNA energy with the conformational energy, one could rely on averaging the effective affinity. In this case, thermodynamic averaging would require taking sample conformations at equal iteration intervals of the SimRNA evolution, this would probably result in a mean effective affinity sensibly different from that represented in Figure 2, with entirely different statistical weights. In Figure 2, the red arrows represent the effective affinity in correspondence of the minimum energy aptamer conformation. Since we referred the aptamer energy conformation to its minimum, on red arrows the effective affinity equals the docking energy.

As already observed, sampling the conformational space brings in many cases to a better evaluation of binding, compared to dock a single reference configuration.

Unfortunately, such differences are to be expected in the present state of the docking art, more important however is the possibility to obtain a similar trend from experimental and simulated binding energies.

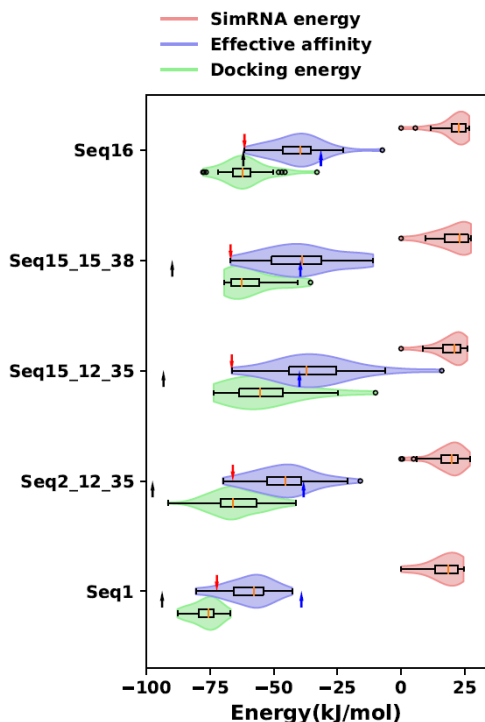


Figure 2. Various computed energy distributions: docking energy (green), SimRNA energy (pink) and effective affinity (violet). Blue arrows represent the experimental ΔG^0 , black arrows the ZRANK values from Hu *et al.* (2015), red arrows the docking energy/effective affinity in correspondence of the most stable aptamer conformation.

An inspection of the experimental binding data shows that sequences Seq1, Seq2_12_35, Seq15_12_35 and Seq15_15_38 behave similarly. The differences among their ΔG^0 , are too small to be reliably reproduced in docking calculations, or by any other computational means; they are also irrelevant to any practical application.

Seq16 instead displays weaker binding. This aspect is well reproduced both in the present calculations and in those by Hu *et al.* (2015), though in the latter case the difference is more evident.

The present calculations however estimate a better binding for Seq1 than for all other sequences, in agreement with the value of the association rate constant calculated in (Hu *et al.*, 2015).

This might well be coincidental, given the small number of aptamers considered, but we would like to advance also two possible causes:

1. wild aptamers could effectively have been engineered by natural selection to span a smaller configurational space;
2. the knowledge-based potential adopted by SimRNA, being obviously based on natural sequences, builds a better potential for wild aptamers, e.g. taking somehow better into account long range interactions (Boniecki *et al.*, 2016).

The different aptamer conformations produced by SimRNA, were then analyzed with respect to their topological and electrical properties. These are powerful tools to identify the mean characteristics of a sequence and to detect extreme structures. On the other hand, once the mean features of each sequence have been recognized, they can be used to make a comparison among sequences.

3.2 Topological properties

To explore the backbone topology of our structures, we calculated the contact map of each realization (Albert *et al.*, 2002) which reproduces the adjacency matrix of the corresponding graph. Inside the same structure, we observed only tiny differences among different realizations, also considering the two choices of RMSD threshold. The mutant aptamers are quite similar, the wild ones Seq1 and Seq16 show a different kind of structure and, in particular, Seq1 has a double folded shape.

A selection of the contact maps, one for each sequence, with two different values of RMSD threshold is reported in Figure 3, for $R_c=10 \text{ \AA}$. The value of the interaction radius has been chosen as the minimum value giving connected networks: In other terms, the mean distance among contiguous nucleobases is about 10 \AA , for all sequences.

The docked structures were also analysed in topology and resistance. In particular, a global information about topology is given by the number of the aptamer-protein-analogue network links: The larger the number of links the closer the aptamer is to the protein.

The link number has been calculated for different R_c values. The Spearman rank correlation has been used to evaluate the results for different values of R_c . It shows a strong and in some cases, very strong monotonic correlation between the link number and the binding energy /effective affinity (See Table 1). The best result is given by $R_c = 20 \text{ \AA}$. Figure 4 reports the corresponding data.

Sequence	Rank Docking energy, $R_c=10\text{\AA}$	Significance Docking energy, $R_c=10\text{\AA}$	Rank Docking energy, $R_c=20\text{\AA}$	Significance Docking energy, $R_c=20\text{\AA}$
1	-0.37	1.1e-1	-0.78	7.1e-4
2_12_35	-0.58	1.5e-4	-0.63	1.3e-4
15_12_35	-0.56	1.1e-2	-0.71	1.2e-3
15_15_38	-0.61	5.4e-2	-0.61	5.4e-2
16	-0.43	2.9e-2	-0.51	9.5e-3
Sequence	Rank EA, $R_c=10\text{\AA}$	Significance EA, $R_c=10\text{\AA}$	Rank EA, $R_c=20\text{\AA}$	Significance EA, $R_c=20\text{\AA}$
1	-0.55	1.7e-2	-0.53	2.1e-2
2_12_35	-0.50	2.5e-3	-0.57	4.8e-4
15_12_35	-0.71	1.6e-3	-0.89	6.4e-5
15_15_38	-0.79	1.3e-2	-0.52	1.0e-1
16	-0.46	1.8e-2	-0.57	3.6e-3

Table 1: Spearman correlation between the docking energy and the effective affinity, for $R_c = 10 \text{ \AA}$ and 20 \AA .

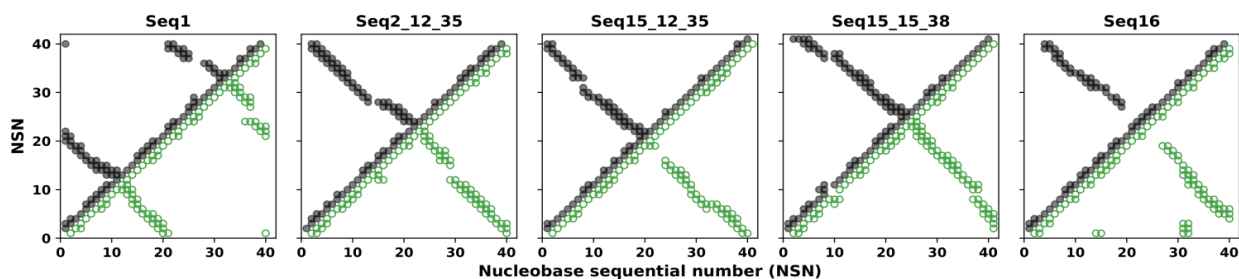


Figure 3. Contact maps for the studied sequences ($R_C=10\text{\AA}$). Dark symbols represent structures with the lowest value of RMDS threshold; light symbols represent structures with the highest value of RMDS threshold.

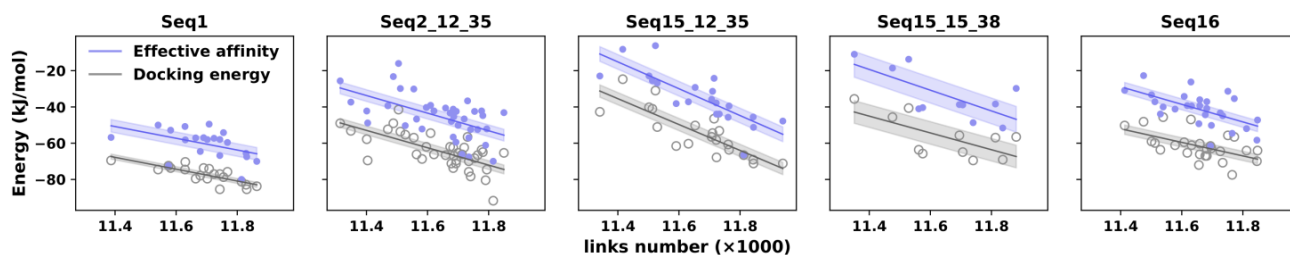


Figure 4. The total number of links vs. docking energy and effective affinity. The interaction radius is $R_C=20\text{\AA}$.

3.3 Electrical properties

A resistance spectrum has been calculated for each realization over an assigned range of R_C values (Alfinito *et al.* 2010, 2011, 2015, 2017).

The resistance spectra, in the R_C range 10-60 \AA , are reported in Figure 5. Each curve represents the average resistance of each aptamer, calculated upon the complete set of realizations. For values of R_C larger than 60 \AA the behaviour does not change significantly, i.e. all the sequences continue to reduce their resistance monotonically. Seq1 is the lowest resistance sequence, in the whole R_C range. This is probably due to its structure which appears as the most complex and connected (see Figure 3), therefore allowing many resistance-parallel connections.

After Seq1, the lowest resistance sequence is the mutant Seq15_15_38. Seq16 is the highest resistance sequence, at small R_C values, whilst Seq2_12_35 is the highest resistance sequence, at the largest R_C values. Resistance depends on the specific structure arrangement and therefore it has been suggested as a computational and experimental tool to evaluate the affinity of aptamers toward their specific target (Alfinito *et al.*, 2017). In the present investigation, the sequences with the lowest and highest resistance correspond to the sequences with the lowest and highest value of the association rate constant, k_{on} , reported by Hu and co-workers (2015). It is interesting to notice that this parallelism between resistance and association rate constant can be stated as it is for the aptamers without the protein, in the pre-docking phase.

Looking at the resistance of the complex, we notice that the mean value of the aptamer-protein complex resistance is quite similar to that of the aptamer alone (Figure 5). This is due to the very different topology of the two biomolecules: the aptamer is made of few nucleobases very far each other, while the protein has many amino acids quite close each other. The result is that, for each R_C value, the protein is much more connected than the aptamer alone and this produces a smaller resistance. The similar response of the aptamer alone and complexed with the appropriate receptor. It is not surprising since most of the information concerning the docking inside the specific structure of the aptamer which was selected exactly for docking that target.

We can also observe that the complex Seq1-Ang2 exhibits the lowest resistance all over the R_C range. On the other side, and as observed for the pre-docking phase, the complexes Seq16-Ang2 and Seq2_12_35-Ang2 are the structures with the highest resistance in the lowest and highest R_C range, respectively, while the other sequences give a very similar response. This result reproduces the trend of the experimental results (Hu *et al.*, 2015).

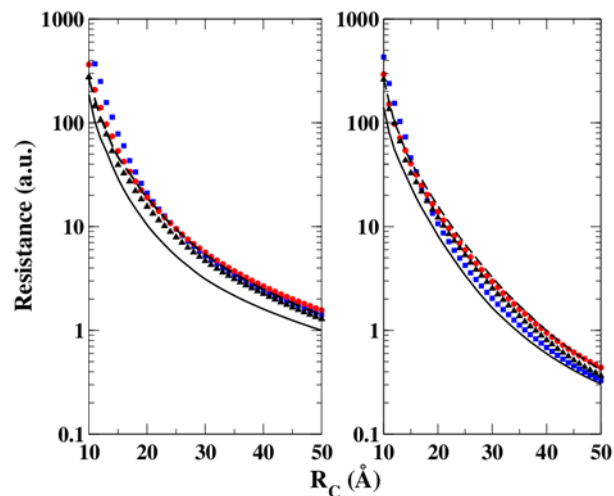


Figure 5. Mean resistance spectra of the 5 selected sequences. On the left, the aptamers in the pre-docking state; on the right, the aptamers complexed with Ang2. Continuous line: Seq1; triangles: Seq15_15_38; dashed line: Seq15_12_35; circles: Seq2_12_35; squares: Seq16.

3.4 PCA analysis on the docked realizations

As an alternate strategy for ranking the *in silico* realizations, we performed some statistical analyses, to provide several possible markers, whose calculation requires low computational resources.

In doing so, the Principal Component Analysis (PCA) was employed, a powerful and common technique for finding patterns in data of high dimension, extensively applied in fields such as face recognition and image compression (Gonzales *et al.*, 1986).

The main advantage is that, once these patterns in the data are found, especially when we have high dimension samples, it is possible to compress the input, i.e. to reduce the number of dimensions, with a modest loss of information in describing the whole system.

In this context, PCA was applied in order to:

- isolate, within a specific sequence, those realizations that contain the major amount of information (characterization);
- identify those realizations that are quite similar from a statistic point of view;
- determine those realizations in which electrical features (resistances) have high correlation with docking energies.

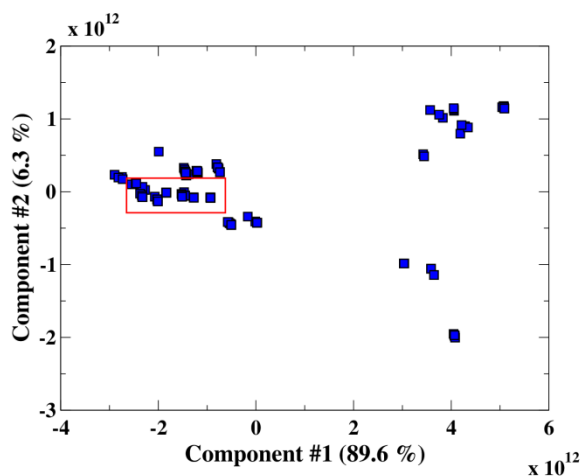


Figure 6. PCA results for the Seq15_12_35. The box indicates the closest representations.

For the considered five sequences, about 600 realizations were obtained after the docking phase. For each realization, a resistance calculation for 100 different R_C values, ranging from 10 to 110 Å was performed. Therefore, it is possible to construct a vector of features comprising the docking energy, called affinity in the AutoDock-Vina log file, together with the RMSD for the lowest and upper bound, the resistivity values, obtained for both the ligand and the ligand-receptor complex, the difference and the relative difference of those resistivities.

For each considered sequence the first component explained over 70% of information, the clusters and/or realizations could be well differentiated; resistances seem to be well correlated with docking energy. Therefore, a shortlist of the closest realizations, in which the electrical features have high correlation with docking energies, can be drawn.

An example is given in Figure 6, where it is evident that the realizations for Seq15_12_35 follow in three macro-areas, with different distances among them. Specifically, the realizations with the less distances are in the clusters: 8, 9, 13, 17, 19. This is a quite useful and powerful tool for evaluating the corpus of realizations of a single aptamer, because it takes into account all the calculated information.

Furthermore, we assessed that the realizations within the same cluster were quite similar, and, for R_C values greater than 20 Å, the principal components do not significantly change, accordingly with the observations highlighted previously.

In conclusion, in this paper we have used a recent method (Boniecki *et al.*, 2016) for the *in silico* generation of the 3D structures of a set of 5 anti-angiopoietin aptamers. The primary structures were given in (Hu *et al.*, 2015) and the docking with Ang-2 was performed by using a set of rigid rotations (Trott *et al.*, 2010).

The analysis of the results was performed with different tests based on the proteotronics approach (Alfinito *et al.*, 2015) which uses an impedance network to describe macromolecules structure and electrical response, in quite agreement with experiments, Seq1 and Seq15_15_38 best perform in resistance so as both Seq 2_12_35 and Seq16 have the highest resistance. Finally the PCA technique allows to select structures which have a similar behavior and which can be used to represent the real aptamer.

Several aspects of the procedure might necessitate further investigation, like the conformational change, the role of solvent, the equal time SimRNA sampling, anyway the ranking provided by the present procedure is in reasonable agreement with experimental data. The method is also reasonably fast and can be easily automated to screen out a large number of aptamer sequences, before experimental measurements.

References

Albert R, Barabasi A L (2002) Statistical mechanics of complex networks, *Reviews of Modern Physics*, 74:47-97

- Alfinito E, Reggiani L (2010) Role of topology in electrical properties of bacterio-rhodopsin and rat olfactory receptor I7. *Physical Review E*, 81(3):032902.
- Alfinito E, Millithaler J-F, Reggiani L, Zine N., Jaffrezic-Renault N, (2011) Human olfactory receptor 17-40 as an active part of a nanobiosensor: a microscopic investigation of its electrical properties. *Rsc Advances*, 1(1):123-127.
- Alfinito E, Pousset J, Reggiani L, (2015) *Proteotronics: Development of Protein-Based Electronics*. (CRC Press).
- Alfinito E, Reggiani L, Cataldo R, De Nunzio G, Giotta L, Guascito M R (2017) Modeling the microscopic electrical properties of thrombin binding aptamer (TBA) for label-free biosensors. *Nanotechnology* 28(6): 065502.
- Baranowski S (2006) *Charge transport in disordered solids with applications in electronics*, ed Baranowski S (Wiley, Chichester, West Sussex)
- Barton W A, Tzvetkova D, Nikolov D B (2005) Structure of the angiopoietin-2 receptor binding domain and identification of surfaces involved in Tie2 recognition. *Structure* 13(5):825-832.
- Bini A, Mascini, M, Turner AP (2011) Selection of thrombin-binding aptamers by using computational approach for aptasensor application. *Biosensors and Bioelectronics*, 26(11): 4411-4416.
- Boniecki M J, Lach G, Wayne K, Dawson W K, Tomala K, Lukasz P, Soltysinski, Rother T K M, Bujnicki J M (2014) SimRNA (version 3.20) User manual, [http:// genesilico. pl/~SimRNA UserManual v3_20_20141002 .pdf](http://genesilico.pl/~SimRNA/UserManual/v3_20_20141002.pdf)
- Boniecki M J, Lach G, Dawson W K, Tomala K, Lukasz P, Soltysinski, Rother T K M, Bujnicki J M (2016) SimRNA: a coarse-grained method for RNA folding simulations and 3D structure prediction. *Nucleic acids research* 44(7): e63-e63.
- Chushak Y, Stone M O (2009) In silico selection of RNA aptamers. *Nucleic acids research* 37(12): e87-e87.
- Doudna J A (2000) Structural genomics of RNA. *Nature Structural & Molecular Biology*, 7(11s):954
- Gilson, M.K. and Zhou, H.X., 2007. Calculation of protein-ligand binding affinities. *Annual review of biophysics and biomolecular structure*, 36.
- Gonzalez R C, Wintz P (1987) *Digital Image Processing* (Addison-Wesley Longman Publishing Co., Inc. Boston, MA, USA, ISBN:0-201-11026-1).
- Hu W P, Kumar J V, Huang C J , Chen W Y (2015) Computational selection of RNA aptamer against angiopoietin-2 and experimental evaluation. *BioMed research international*, 2015. <http://dx.doi.org/10.1155/2015/658712>
- Kitchen D B, Decornez, H, Furr, J R, Bajorath, J (2004) Docking and scoring in virtual screening for drug discovery: methods and applications. *Nature reviews. Drug discovery* 3(11): 935.
- Kinnings S L, Liu N, Tonge P J, Jackson R M, Xie L, Bourne P E (2011) A machine learning based method to improve docking scoring functions and its application to drug repurposing. *J Chem Inf Model*. 51(2): 408–419, doi: 10.1021/ci100369f.
- Lee J W, Kim H J, Heo K (2015) Therapeutic aptamers: developmental potential as anticancer drugs. *BMB reports*, 48(4): 234.
- Rother K, Rother M, Boniecki M, Puton T, Bujnicki J M (2011) RNA and protein 3D structure modeling: similarities and differences. *Journal of molecular modeling*, 17(9):2325-2336.
- Stewart A A, McCammon J A (2006) Molecular Dynamics: Survey of methods for simulating the activity of proteins. *Chem. Rev.* 106(5):1589-1615.
- Piazza F, De Los Rios P, Cecconi F (2009) Temperature dependence of normal mode ons of protein dynamics. *Physical Review Letters*, 102(21): 218104.
- Tirion M M (1996) Large amplitude elastic motions in proteins from a single-parameter, atomic analysis. *Physical review letters*, 77(9): 1905.
- Trott O, Olson A J (2010) AutoDock-Vina: improving the speed and accuracy of docking with a new scoring function, efficient optimization, and multithreading. *J. computational chemistry*, 31(2),455-461.
- Tuerk C, Gold, L (1990) Systematic evolution of ligands by exponential enrichment: RNA ligands to bacteriophage T4 DNA polymerase. *Science*, 249(4968):505-510.
- Yüce M, Ullah N, Budak H (2015) Trends in aptamer selection methods and applications. *Analyst*, 140(16): 5379-5399.

